Interfacial Reactivity of Hydroxyl-Terminated Monolayers in the Absence of Solvents

Rajaram C. Sabapathy and Richard M. Crooks*

Department of Chemistry, Texas A&M University, P.O. Box 30012, College Station, Texas 77842-3012

Received July 13, 1999. In Final Form: October 13, 1999

We compare the interfacial reactivity between vapor- or liquid-phase heptanoyl chloride (C_6COCl) and hydroxyl-terminated monolayers prepared from 4-hydroxythiophenol (HTP), 11-mercaptoundecanol (MUD), and a hydroxyl-terminated, fourth-generation poly(amidoamine) (PAMAM) dendrimer (G4-OH). Fourier transform infrared−external reflection spectroscopy indicates that both vapor- and liquid-phase C_6COCl reacts with all three hydroxyl-terminated self-assembled monolayers (SAMs) to yield ester-coupled bilayers. The spectroscopic data were confirmed by contact-angle goniometry, which revealed advancing contact-angle increases of between 60 and 75° after vapor-phase reaction, and ellipsometric measurements, which indicated that the films increased in thickness by 0.4−0.6 nm. Similar results were obtained when the ester-coupling reaction was carried out in liquid-phase CH_2Cl_2. Real-time, quantitative surface acoustic wave (SAW)-based nanogravimetry indicates that the vapor-phase reactions go to completion in <1 min. The order of reactivity of the monolayers decreases in the order G4-OH > MUD > HTP. This is interpreted in terms of monolayer structure and the intrinsic properties of the particular coupling reaction studied.

Introduction

In this report we compare the interfacial reactivity between vapor- or liquid-phase heptanoyl chloride (C_6-COCl) and hydroxyl-terminated monolayers prepared from 4-hydroxythiophenol (HTP), 11-mercaptoundecanol (MUD), and a hydroxyl-terminated, fourth-generation poly(amidoamine) (PAMAM) dendrimer (G4-OH) (Scheme 1). The objective of this study is to begin the process of systematically developing an understanding of the factors influencing organic synthesis in the absence of solvents. Such conditions offer promise for studying and finding technological uses for reactions that do not proceed in the presence of liquid solvents or are adversely affected by the presence of solvent.[1] Moreover, solvent-free processes lend themselves to automation and eliminate the need for solvent remediation.[2]

Thus far, our work in this area has focused on demonstrating the feasibility of using vapor-phase reactants to carry out chemical reactions on self-assembled monolayers[3] (SAMs) of ω-functionalized organomercaptans confined to Au substrates. For example, we previously reported real-time measurements of the coupling reaction between surface-confined monolayers of HTP and vapor-phase dimethyloctylchlorosilane.[4] Fourier transform infrared−external reflection spectroscopy (FTIR−ERS) demonstrated that this reaction yields a new siloxane bond in the linked bilayer, and surface acoustic wave (SAW)-based nanogravimetry indicated that the reaction proceeded rapidly and quantitatively. This system provides a good model for studying the reactivity of silanes at hydroxylated surfaces such as those that can be formed on glass and many metal oxides.[3] Hydrogen-bonded[5] and electrostatically bonded[6,7] bilayers can also be quantitatively formed at the solid/vapor interface. For example, alkanoic acids can self-assemble onto acid-functionalized organomercaptans.[5] Similarly, primary amines self-assemble onto

Scheme 1

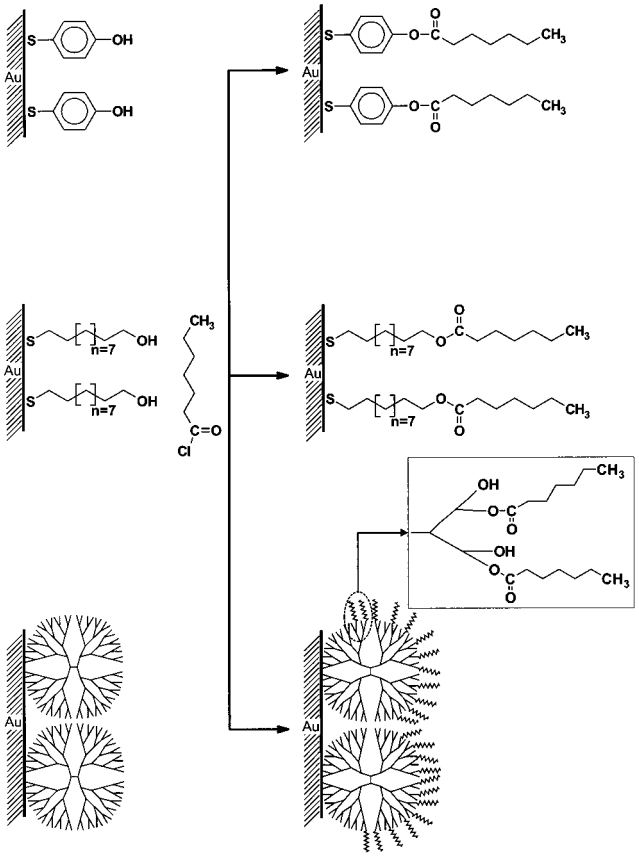

* To whom correspondence should be addressed. (E-mail: crooks@tamu.edu; voice: 409-845-5629; fax: 409-845-1399).

(1) Sun, L.; Crooks, R. M.; Ricco, A. J. *Langmuir* **1993**, *9*, 1775.
(2) Raber, L. *Chem. Eng. News* **1998**, *76*, 6(38), 39.
(3) Ulman, A. *Chem. Rev.* **1996**, *96*, 1533, and references therein.
(4) Sun, L.; Thomas, R. C.; Crooks, R. M.; Ricco, A. J. *J. Am. Chem. Soc.* **1991**, *113*, 8550.
(5) Sun, L.; Kepley, L. J.; Crooks, R. M. *Langmuir* **1992**, *8*, 2101.
(6) Yang, H. C.; Dermody, D. L.; Xu, C.; Ricco, A. J.; Crooks, R. M. *Langmuir* **1996**, *12*, 726.
(7) Wells, M.; Dermody, D. L.; Yang, H. C.; Kim, T.; Crooks, R. M.; Ricco, A. J. *Langmuir* **1996**, *12*, 1989.

10.1021/la990936p CCC: $19.00
Published on Web 12/10/1999

acidic monolayers via a strong electrostatic interaction following proton transfer from the acid to the vapor-phase base.[6,7]

In addition to our own work, a number of other studies have appeared that demonstrate alternative approaches for linking vapor-phase reactants and ω-functionalized SAMs.[8−13] For example, functionalization of hydroxyl- and acid-terminated SAMs with vapor-phase anhydrides is an especially promising strategy.[8,9] Corn and co-workers carried out the derivatization of surface-confined carboxylic acid groups by activation with vapor-phase thionyl chloride and subsequent reaction with different amines and alcohols.[10] The reaction between vapor-phase phenyl isocyanate and hydroxyl- and acid-terminated SAMs has been studied under ultrahigh vacuum (UHV) conditions, but no reaction occurs at room temperature.[11] Although vapor-phase reactions with less well-defined substrates have also been described,[12,13] to the best of our knowledge these are the only examples of reactions between organic monolayers and vapor-phase reactants.

It is possible to draw a number of conclusions from the aforementioned studies. First, there are a number of successful strategies for preparing covalently linked bilayers from organic monolayers and vapor-phase reactants. In addition, such reactions may proceed rapidly and go to completion. Second, the reactants must have sufficient vapor pressure under the experimental conditions to reach the monolayer surface. A particularly successful strategy for ensuring sufficient vapor pressure at room temperature and atmospheric pressure has been to fully or partially fluorinate the vapor-phase reactant. Third, reaction byproducts must have sufficient vapor pressure that condensation is precluded and the byproducts must not react with the reactants to yield a low-vapor-pressure contaminant, such as an ammonium salt. Fourth, surface reactions must proceed in the absence of catalysts and thus may be limited to simple substitution- or addition-type reactions.

In this study, the base monolayers (HTP, MUD, and G4-OH) were prepared on Au substrates from ethanolic solutions. The monolayer-modified Au substrates were then exposed to the acid chloride vapor diluted in a flowing stream of dry N_2. This results in the formation of bilayer assemblies coupled via ester linkages (Scheme 1). The byproduct of this reaction is gaseous HCl that is removed from the monolayer surface in the N_2 stream. For comparison, this same coupling chemistry was also carried out in liquid-phase solvents. Finally, the substrates were characterized before and after linking using contact-angle measurements,[14,15] ellipsometry,[16] FTIR−ERS,[17] and SAW-based nanogravimetry[18] to determine the extent of reaction and the chemical and physical properties of the resulting bilayer.

Experimental Section

Chemicals. The following chemicals were purchased from the Aldrich Chemical Co. (Milwaukee, WI) and used as received: MUD, 97%; C_6COCl, 99%; dichloromethane, 99.8%; acetonitrile, 99.8%; and pyridine, 99.8%. HTP (Aldrich, 90%) was purified by vacuum sublimation before use. Fourth-generation, hydroxyl-terminated poly(amidoamine) dendrimers (G4-OH) (51% w/w, MeOH) (Dendritech, Inc., Midland, MI) and 100% ethanol (Quantum Chemical Co., Tuscola, IL) were used as received. Water was purified (resistivity ≥ 18 MΩ-cm) using a Milli-Q reagent water system (Millipore, Bedford, MA). N_2 from gas cylinders had a purity of at least 99.995% and was passed through two Drierite gas drying units (Hammond 26800, Fisher Scientific Co., Pittsburgh, PA) before use.

Substrates. Au-coated substrates were prepared by electron-beam deposition of 10 nm of Ti followed by 200 nm of Au onto Si(100) wafers (Lance Goddard Associates, Foster City, CA).[7] The wafers were subsequently diced into 2.6 cm × 1.3 cm pieces. SAW devices were coated with Au in the same manner on polished ST-cut quartz (Lance Goddard).[6]

Procedures. Before each experiment all wafers and SAW devices were cleaned in a low-energy ozone cleaner for 10 min (model 135500, Boekel Industries, Inc.). Diced wafers and SAW devices were rinsed with warm ethanol for 1−2 min and then soaked for >18 h in either an ethanolic 1 mM solution of HTP or MUD, or in a 0.1 mM ethanolic solution of G4-OH. After they were removed from the soaking solution, the substrates were rinsed with ethanol, sonicated for 1−2 min in ethanol to remove physisorbed material, rinsed with ethanol again, and then dried in a stream of N_2. The base-layer-modified Au substrates were analyzed by contact-angle and ellipsometric measurements, as well as FTIR−ERS, prior to vapor- or liquid-phase functionalization.

Vapor-Phase Functionalization. Immediately after base-layer modification, the substrates were transferred to a clean borosilicate glass vial fitted with a Teflon/silicone septum. This vessel was purged with N_2 for at least 20 min prior to dosing with the vapor-phase reactants. Vapor-phase C_6COCl was generated by passing N_2 at 0.25 L/min over the headspace of a vial containing neat liquid C_6COCl. The resulting subsaturated vapor was passed over the base-layer-modified substrate via a 1.5 mm i.d. Teflon tube for 20−30 min. Excess reactant was removed from the reaction vial and substrate surface by purging with pure N_2 for 20 min prior to bilayer characterization. FTIR−ERS spectra were obtained immediately after purging with N_2 and again after sonicating and rinsing with CH_2Cl_2 or CH_3CN to ensure covalent linking of the bilayer and removal of physisorbed material. Naked Au substrates were also dosed with the vapor-phase reactants and rinsed as described above to ensure that this protocol completely removed physisorbed reactants. All vapor-phase functionalization experiments were carried out at 23 ± 2 °C.

Liquid-Phase Functionalization. Bilayers were also prepared by liquid-phase reaction. For these studies Au substrates modified with the base monolayers were immersed in a 0.1 M solution of C_6COCl in dry CH_2Cl_2 containing an excess (0.2 M) of dry pyridine. The progress of the reaction was checked by FTIR−ERS every 10 min for an hour, and the spectra stopped changing after 20 min. The spectra shown in this paper were obtained after a reaction period of 30 min. For the vapor-phase experiments, a naked Au substrate served as a control. The liquid-phase reactions were carried out at 23 ± 2 °C.

FTIR−ERS. FTIR−ERS measurements were made using a Digilab FTS-40 spectrometer (Bio-Rad, Cambridge, MA) equipped with a Harrick Scientific Seagull reflection accessory (Ossining, NY) and a liquid-N_2-cooled mercury cadmium telluride (MCT) detector. All spectra were the sum of 256 individual scans and obtained at 4 cm^{-1} resolution using *p*-polarized light at an 84° angle of incidence with respect to the Au substrate.[6]

Ellipsometric Thickness Measurements. Ellipsometric measurements were made in air with a Gaertner Scientific (Chicago, IL) model L2W26D ellipsometer using a 70.00 ± 0.02° angle of incidence, 632.8 nm laser light, and assuming a film refractive index (n_f) of 1.46. The reported thicknesses are the average of 25 measurements made at five different locations on each of five independently prepared substrates. The estimated error in the thickness measurements is ±0.3 nm.

(8) Hutt, D. A.; Leggett, G. J. *Langmuir* **1997**, *13*, 2740.
(9) Pan, S.; Castner, D. G.; Ratner, B. D. *Langmuir* **1998**, *14*, 3545.
(10) Duevel, R. V.; Corn, R. M. *Anal. Chem.* **1992**, *64*, 337.
(11) Himmel, H.-J.; Weiss, K.; Jäger, B.; Dannenberger, O.; Grunze, M.; Wöll, Ch. *Langmuir* **1997**, *13*, 4943.
(12) Matsuura, K.; Ebara, Y.; Okahata, Y. *Langmuir* **1997**, *13*, 814.
(13) Evenson, S. A.; Badyal, J. P. S. *J. Phys. Chem. B* **1998**, *102*, 5500.
(14) Bain, C. D.; Troughton, E. B.; Tao, Y.-T.; Evall, J.; Whitesides, G. M.; Nuzzo, R. G. *J. Am. Chem. Soc.* **1989**, *111*, 321.
(15) Bain, C. D.; Evall, J.; Whitesides, G. M. *J. Am. Chem. Soc.* **1989**, *111*, 7155.
(16) Folkers, J. P.; Laibinis, P. E.; Whitesides, G. M. *Langmuir* **1992**, *8*, 1330.
(17) Crooks, R. M.; Xu, C.; Sun, L.; Hill, S. L.; Ricco, A. J. *Spectroscopy* **1993**, *8*, 28, and references therein.
(18) Ricco, A. J. *Electrochem. Soc. Interface* **1994**, *3*, 38.

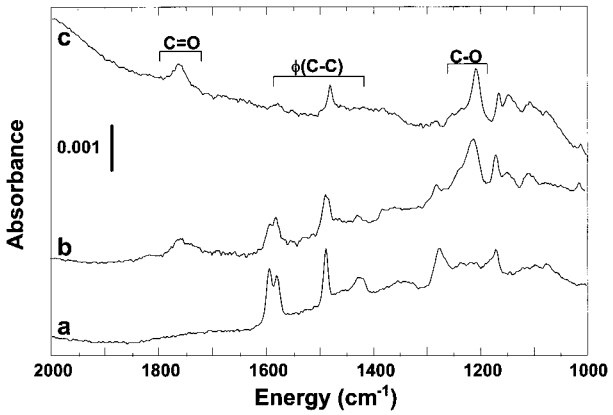

Figure 1. FTIR−ERS spectra of (a) an HTP monolayer; (b) an HTP monolayer after exposure to vapor-phase C_6COCl; and (c) an HTP monolayer after exposure to a solution of CH_2Cl_2 containing C_6COCl and pyridine.

Contact-Angle Measurements. Advancing water contact angles were measured using an FTA-200 goniometer (First Ten Angstroms, Portsmouth, VA) and double-distilled water. The stage holding the substrate was housed in a transparent enclosure to minimize exposure of the Au surface to the surroundings. The reported thicknesses are the average of 25 measurements made at five different locations on each of five independently prepared substrates. The estimated contact-angle error is ±5°.

SAW Device-Based Nanogravimetry. SAW device measurements were made at 22 ± 1 °C using two ST-cut quartz oscillators housed in a custom built flow system.[6,19] Modified SAW devices were dosed with ~25%-of-saturation C_6COCl vapor diluted in N_2 (flow rate, 0.5 L/min). In the thin-film limit, the change in SAW-device frequency (Δf) is related to the mass loading per unit area (m_a) through the equation $\Delta f/f_0 = -\kappa c_m f_0 m_a$, where f_0 is the SAW resonance frequency (96 MHz), κ is the fraction of the distance between the centers of the transducers covered by the chemically modified Au film (0.7), and c_m is the mass-sensitivity coefficient of the device (1.33 $cm^2/g \cdot Hz$) for ST-cut quartz.[18,19] All surface concentrations are corrected for a surface roughness factor of 1.2 ± 0.2.[6,7,19] The dosing experiments were repeated at least four times on independently prepared SAW devices and the results were found to be within ±1 ppm of the average value of Δf.

Results and Discussion

Figure 1 shows FTIR−ERS spectra of an HTP monolayer before (spectrum a) and after vapor-phase (spectrum b) and liquid-phase (spectrum c) derivatization with C_6COCl. The spectrum of the base HTP monolayer prior to dosing reveals peaks at 1594, 1579, 1487, and 1428 cm^{-1} that are characteristic of the HTP aromatic ring.[4] After dosing with vapor-phase C_6COCl these bands change slightly, and two new bands are apparent at 1760 and 1250 cm^{-1}, which are assigned to the ν(C═O) and ν(C−O) modes, respectively, of the new ester-linked bilayer (Scheme 1).[20] When the same reaction is carried out in liquid CH_2Cl_2 a very similar spectrum results, which confirms, at least qualitatively, that this reaction proceeds similarly in liquid and vapor phases.

A careful comparison of all three spectra in Figure 1 indicates significant differences in the position and magnitude of the ring-derived IR bands depending on how the coupling reaction is carried out. For example, the spectrum obtained after liquid-phase coupling reveals near-complete disappearance of the bands at 1594 and 1579 cm^{-1}, arising from quadrant stretching modes of the ring, and the band at 1428 cm^{-1}, which is attributed to a semicircle stretch.[20] Compared to the HTP-only monolayer, similar but less dramatic changes in these same bands are evident when the bilayer is prepared in solvent-free conditions. We attribute these spectral differences to reaction-induced changes in the orientation of the HTP ring.[17] There is another interesting aspect of Figure 1: the ester C−O band intensity is significantly stronger than that of the C═O band, whereas the relative magnitude of these two bands is usually reversed in bulk-phase IR spectra of esters.[21] We ascribe this result to the high degree of orientation of this bond within the bilayer:[22,23] although the C−O oscillator strength is weaker than C═O, the surface-parallel orientation of the latter greatly reduces its intensity, whereas the opposite is true for C−O. Note that no additional changes in the spectra shown in Figure 1 were observed after the monolayers were rinsed and sonicated in CH_2Cl_2 or CH_3CN, which indicates that simple N_2 purging removes whatever unreacted, physisorbed C_6COCl might remain on the surface after dosing. This result has important consequences for the nanogravimetric data discussed later.

Table 1. Contact-Angle, Ellipsometric Thickness, and Nanogravimetric Data for Monolayers and Bilayers Prepared by Vapor- and Liquid-Phase Reaction between C_6COCl and HTP, MUD, and G4-OH Monolayers

base monolayer	contact-angle (deg)[a] initial	vapor	liquid[d]	film thickness (nm)[b] initial	vapor	liquid[d]	mass[c] (ng/cm^2)
Au only	<10	<10	<10	–	–	–	–
Au/HTP	20	95	105	0.6	1.0	1.1	48 ± 7
Au/MUD	15	90	95	1.2	1.6	1.7	61 ± 5
Au/G4-OH	15	75	85	1.6	2.2	2.3	44 ± 8

[a] Average of five advancing water contact-angle (θ_a) measurements made on each of five independently prepared substrates. [b] Average of five different ellipsometric thickness measurements made at five different locations on each of five independently prepared substrates. [c] Change in mass before and after exposure of the base layer to vapor-phase C_6COCl. The value shown is the average of four measurements made on independently prepared SAW devices after correcting for a surface roughness factor of 1.2. [d] Prepared in a CH_2Cl_2 solution containing 0.1 M C_6COCl and 0.2 M pyridine.

The FTIR−ERS results shown in Figure 1 indicate at least partial esterification of the hydroxyl-terminated HTP monolayer upon reaction with vapor-phase C_6COCl, and ellipsometric-thickness and contact-angle measurements confirm this finding (Table 1). Prior to reaction the HTP monolayer has a contact angle of 20°, which confirms that the hydrophilic hydroxyl group is exposed at the monolayer surface. However, the contact angle increases to 95 or 105° after reaction with vapor- or liquid-phase C_6COCl, respectively. The corresponding ellipsometric thicknesses increase after reaction by 0.4 and 0.5 nm. These values are somewhat lower than the 0.75 nm increase expected for an all-trans, extended seven-carbon chain.[24] This suggests incomplete reaction, a tilted orientation of the bilayer, gauche defects, error in the ellipsometric thickness measurements, or (most likely) a combination of all four effects. However, the important point is that there is a significant and reproducible increase in the thickness and

(19) Dermody, D. L.; Crooks, R. M.; Kim, T. *J. Am. Chem. Soc.* **1996**, *118*, 11912.
(20) Colthup, N. B.; Daly, L. H.; Wiberley, S. E. *Introduction to Infrared and Raman Spectroscopy*; Academic: Boston, 1990.
(21) Silverstein, R. M.; Bassler, G. C.; Morrill, T. C. *Spectrometric Identification of Organic Compounds*, 4th ed.; John Wiley: New York, 1991.
(22) Ryswyk, H. V.; Turtle, E. D.; Watson-Clark, R.; Tanzer, T. A.; Herman, T. K.; Chong, P. Y.; Waller, P. J.; Taurog, A. L.; Wagner, C. E. *Langmuir* **1996**, *12*, 6143.
(23) Engquist, I.; Lestelius, M.; Liedberg, B. *Langmuir* **1997**, *13*, 4003.
(24) Calculated using Cerius^2 3.0, Molecular Simulations, Inc., San Diego, CA, 1997.

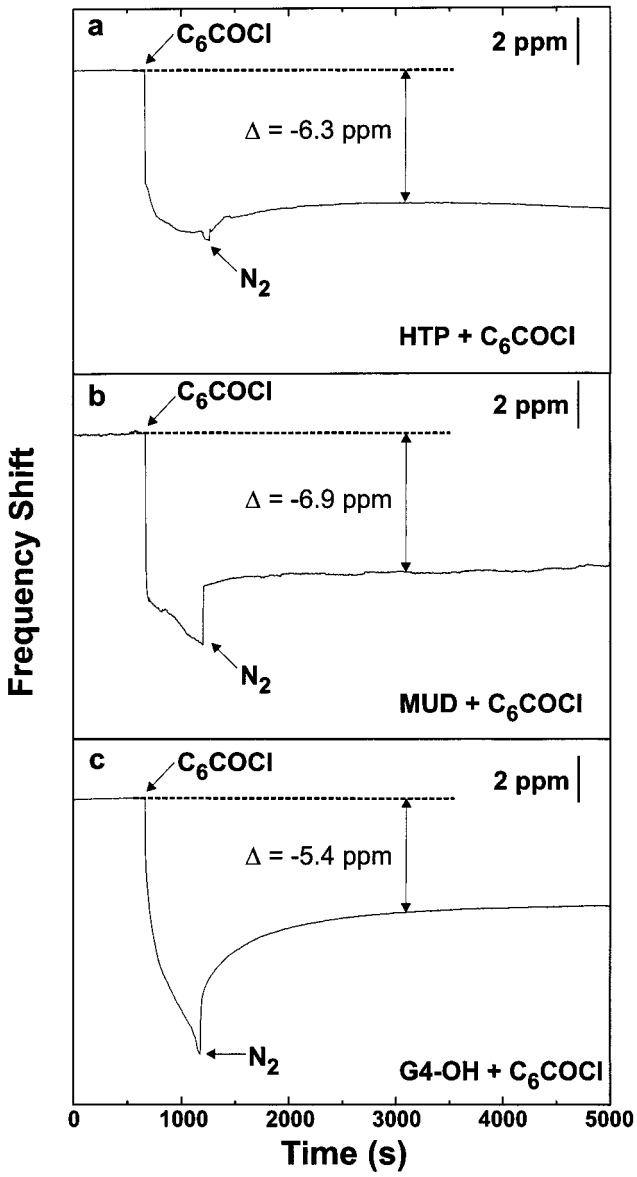

Figure 2. Representative in-situ SAW device frequency responses obtained for dosing monolayers of (a) HTP, (b) MUD, and (c) G4-OH with ~25%-of-saturation C_6COCl vapor mixed with dry N_2.

contact-angle of the bilayer film after reaction, which is fully consistent with addition of the ester-coupled hydrocarbon. Moreover, the magnitude of the increase is about the same regardless of whether the reaction is carried out in the vapor or liquid phase.

Part a of Figure 2 provides typical, quantitative, unprocessed nanogravimetric data corresponding to the HTP/C_6COCl coupling reaction. These data were obtained by dosing an HTP-modified SAW device with ~25%-of-saturation C_6COCl vapor diluted in N_2. At the beginning of the experiment the SAW device was purged with N_2 until the frequency stabilized. Next, the HTP surface was exposed to ~25%-of-saturation C_6COCl vapor for 500−600 s and then purged with N_2 for >3000 s until the baseline stabilized. The just-discussed IR data indicate that N_2 purging removes all physisorbed C_6COCl, so we are confident that the observed frequency response corresponds nearly exclusively to covalently linked reactant. This experiment was carried out four times on independently prepared SAW devices, and the average change in frequency (Δf) before and after exposure to C_6-

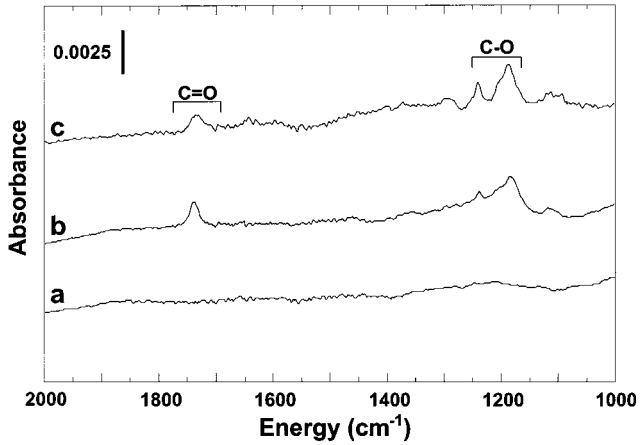

Figure 3. FTIR−ERS spectra of (a) a MUD SAM; (b) a MUD SAM after exposure to vapor-phase C_6COCl; and (c) a MUD monolayer after exposure to a solution of CH_2Cl_2 containing C_6COCl and pyridine.

COCl was 5.1 ± 1.2 ppm (note: the data shown in the figure correspond to just one of the four trials), which corresponds to 48 ± 7 ng/cm^2 (0.43 ± 0.06 nmol/cm^2) after taking into account the Au surface roughness factor of 1.2. If we assume monolayer coverage of HTP,[7,19] this mass corresponds to 55% of the surface-confined HTP reacting with C_6COCl vapor. This can be compared to the reaction between surface-confined HTP and vapor-phase $[CH_3(CH_2)_7](CH_3)_2SiCl$, which we previously showed went to completion.[4] Thus, the low reactivity observed for the HTP/C_6COCl esterification reaction is not inherent to the chemical or structural motif of the HTP monolayer, but rather is governed by the vapor-phase reactant. Moreover, because the structures of both C_6COCl and $[CH_3(CH_2)_7](CH_3)_2SiCl$ are dominated by very similar hydrocarbon moieties, we propose that the differences in reactivity are mostly due to mechanistic differences between the silanization and esterification reactions.

To better understand how the chemical and structural properties of the base monolayer affect this ester coupling reaction, we compared the just-described results for the aromatic alcohol to a base monolayer composed of the aliphatic alcohol MUD. FTIR−ERS results confirming coupling between MUD and C_6COCl are shown in Figure 3. Prior to reaction no distinct bands are observed in the spectral region shown in spectrum a, but bands at 2923 and 2852 cm^{-1} (not shown) which we attribute to asymmetric and symmetric methylene bands, respectively, confirm the presence of MUD on the Au substrate. After exposure of the MUD base monolayer to vapor- or liquid-phase C_6COCl, two new bands at 1740 and 1250 cm^{-1} are apparent (spectra b and c, respectively). As for the HTP/C_6COCl coupling reaction, these bands correlate to the formation of a new ester bond (middle frame of Scheme 1).

In addition to the aforementioned spectral changes, there is also an increase in the contact angle before (15°) and after (90 and 95° for vapor- and liquid-phase reactions, respectively) coupling. These values are slightly lower than observed for coupling to the aromatic HTP monolayer, which perhaps signals a slightly less ordered bilayer or a somewhat less complete reaction on MUD. The thickness increases after coupling are identical to those measured for HTP (Table 1).

The nanogravimetric data obtained for the coupling reaction are shown in part b of Figure 2. The average frequency change before and after exposure to C_6COCl is 6.5 ± 0.6 ppm, which corresponds to 61 ± 5 ng/cm^2 (0.54

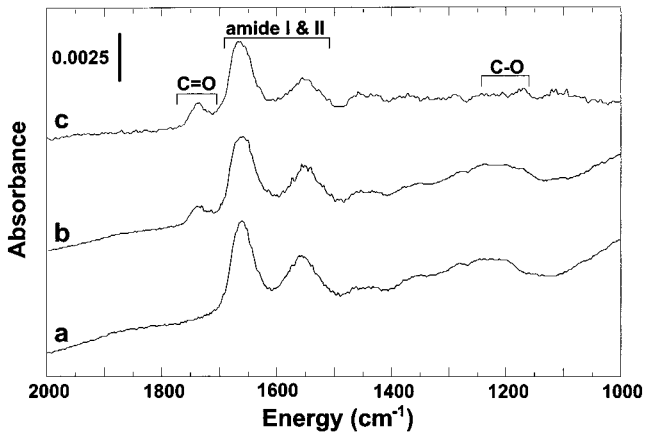

Figure 4. FTIR−ERS spectra of (a) a G4-OH monolayer; (b) a G4-OH monolayer after exposure to vapor-phase C_6COCl; and (c) a G4-OH monolayer after exposure to a solution of CH_2Cl_2 containing C_6COCl and pyridine.

± 0.05 nmol/cm^2). These values indicate that about 69% of the surface-confined MUD reacts with C_6COCl, which is ∼1/3 higher than was measured for the HTP-modified surface. Because the surface concentrations of HTP and MUD are identical,[4] we conclude that the terminal hydroxyl group of MUD is more sterically accessible for esterification. The hydroxyl group of HTP is most likely oriented perpendicular to the Au surface,[4,7] while that of MUD is canted and probably is also more free to move into a reactive configuration.

Both HTP and MUD form relatively ordered monolayers on the surface of Au,[4,25] and we thought it would be interesting to compare the reactivity of these ordered systems to one that is intrinsically disordered. Accordingly, we examined the reactivity between C_6COCl and a monolayer prepared from a fourth-generation, PAMAM dendrimer having 64 terminal hydroxyl groups (G4-OH). G4-OH compresses to an oblate conformation on Au and forms stable, densely packed monolayers via polydentate interactions between interior tertiary amine groups of the dendrimer and the Au surface.[26]

Spectrum a in Figure 4 shows an FTIR−ERS spectrum of a G4-OH monolayer on a Au substrate. The amide I and II peaks at 1660 and 1550 cm^{-1}, which arise from the dendrimer branches, confirm immobilization.[26] Following derivatization with vapor- and liquid-phase C_6COCl (spectra b and c of Figure 4, respectively), a small band corresponding to the new ester bond is apparent at 1740 cm^{-1}. However, in contrast to the data for HTP and MUD, there is no clearly defined peak around 1250 cm^{-1} corresponding to the ester C−O bond. This suggests that the postulated orientation-induced enhancement of this band observed for the two ordered SAMs is absent here, which is consistent with the disordered nature of the dendrimer base layer and the roughly spherical symmetry of the dendrimer. We conclude that ordered base layers give rise to relatively well-ordered bilayers and that disordered base layers give rise to disordered bilayers having multiple orientations (bottom frame of Scheme 1).

As for HTP and MUD, an increase in the contact angle and film thickness results after the coupling reaction between C_6COCl and G4-OH (Table 1). Consistent with the FTIR−ERS data, which suggest that the dendrimer monolayer is capped with a disordered alkyl-terminated bilayer, the magnitude of this contact angle increase is not as large as that for HTP and MUD. Rather, the contact angle increases from an initial value of 15 to 75 and 85° for the vapor- and liquid-phase reactions, respectively. It is likely that these lower contact angles arise in part from unreacted hydroxyl groups near the surface of the dendrimers and in part from the general disorder inherent to the dendrimer-supported bilayer.

The G4-OH film thicknesses increase by 0.6 and 0.7 nm for the vapor- and liquid-phase reactions, respectively. The similarity between these results and those found for the other two SAMs (Table 1) is likely somewhat fortuitous given the nonuniform structure of the dendrimer films. Moreover, the model we used for interpreting the ellipsometric data assumes that the film is composed of a homogeneous slab, which is only a rough approximation for surface-confined dendrimers.[26] Part c of Figure 2 shows nanogravimetric data corresponding to the G4-OH/C_6-COCl coupling reaction. The observed average frequency change is 4.7 ± 0.9 ppm, which after accounting for the roughness factor corresponds to 44 ± 8 ng/cm^2 (0.39 ± 0.08 nmol/cm^2).

The SAW data provide a reasonable means for estimating the percentage of reactive hydroxyl groups on the dendrimer-modified surface. From a previous study we know the surface coverage of G4-OH is quite high: about 92%.[26] Taking into account the size of the oblate, surface-confined dendrimer (6.3 nm in diameter),[26] this corresponds to a surface concentration of 4.8 pmol/cm^2, and because there are 64 terminal groups per G4-OH, the surface concentration of hydroxyl groups is 0.31 nmol/cm^2. Given the three-dimensional structure of the dendrimers, it is somewhat surprising that this value is actually less than the surface concentration of hydroxyl groups in the strictly two-dimensional MUD and HTP SAMs (0.78 nmol/cm^2).

Certain factors unique to dendrimers make it difficult to estimate the percentage of terminal groups that react. For example, if we assume that the entire measured mass change corresponds to addition of C_6COCl, then, under the set of assumptions described in the previous paragraph, 125% of the surface hydroxyl groups react. This is clearly an unphysical value. One reasonable explanation for this finding is that some C_6COCl irreversibly chemisorbs within the dendrimer interior, but we view this as unlikely because most unreactive volatile organic compounds sorb reversibly.[27−29] A more likely explanation is that some HCl generated as a byproduct of the reaction complexes with interior tertiary amine groups of the dendrimer. In this case, the effective molecular weight of the reactant increases from 112 to 149 g/mol, and this lowers the percentage reactivity of the surface hydroxyl groups to 95%. Because it is rather unlikely that all HCl is scavenged and that all hydroxyl groups are exposed to the reactant (some are likely tucked inside the dendrimer,[30] while others are sterically crowded by the Au surface or nearby dendrimers), we conclude that essentially all of the dendrimer surface groups react. Given the significantly lower reactivity of the two SAMs, it seems reasonable to conclude that close-packed, organized monolayers are less reactive than the disordered dendrimer terminal groups.

(25) Karpovich, D. S.; Blanchard, G. J. *Langmuir* **1997**, *13*, 4031.
(26) Tokuhisa, H.; Zhao, M.; Baker, L. A.; Phan, V. T.; Dermody, D. L.; Garcia, M. E.; Peez, R. F.; Crooks, R. M.; Mayer, T. M. *J. Am. Chem. Soc.* **1998**, *120*, 4492.
(27) Wells, M.; Crooks, R. M. *J. Am. Chem. Soc.* **1996**, *118*, 3988.
(28) Osbourn, G. C.; Ricco, A. J.; Bartholomew, J. W.; Martinez, R. F.; Garcia, M. E.; Peez, R.; Crooks, R. M.; Spindler, R.; Kaiser, M. E. *Technical Digest of the 1998 Solid-State Sensor and Actuator Workshop*, Hilton Head Island, SC, June 1998; Transducer Research Foundation, Cleveland, 1996.
(29) Tokuhisa, H.; Crooks, R. M. *Langmuir* **1997**, *13*, 5608.
(30) Lescanec, R. L.; Muthukumar, M. *Macromolecules* **1990**, *23*, 2280.

Summary and Conclusions

In summary, we compared the reactivity of three hydroxyl-terminated monolayers (HTP, MUD, and G4-OH) with vapor- and liquid-phase C_6COCl. All three monolayers react to form ester-coupled bilayers. The extent of reactivity decreases in the order G4-OH > MUD > HTP. Although it is somewhat presumptuous to draw generalizations from such a limited data set, it does seem that highly ordered monolayers (HTP and MUD) are less reactive than disordered systems (the dendrimer), and that monolayers with more flexible reactive groups (MUD) are more reactive than those held rigidly (HTP). On the basis of our previous work with silane coupling reactions,[4] we also conclude that the intrinsic reactivity of the reactants (that is, the mechanistic details of how the reaction occurs) impact the extent of reaction. Finally, spectroscopic, ellipsometric, and contact-angle measurements suggest that the chemical and physical properties of the bilayers do not depend very strongly on whether they are prepared in the vapor or liquid phase. However, the FTIR−ERS results do suggest that there are subtle differences in the molecular orientation of the bilayers depending on how the reactions are carried out.

Our approach for synthesizing organic thin films in the absence of solvents has been limited thus far to two layers. We recently extended this to three and more layers, and the results of those experiments will be reported soon. As we learn more about the rules governing organic chemistry at vapor/solid interfaces, we believe this general approach will find use as a general synthetic method for preparing functional thin films having technological applications.

Acknowledgment. We gratefully acknowledge the U. S. Department of Energy (Advanced Energy Projects, Contract DE-FG03-97ER12212) for full support of this work. We acknowledge Dr. Li Sun for helpful discussions. We also thank Mr. Mark Kaiser (Dendritech, Inc., Midland, MI) for providing technical information and supplying the amine-terminated Starburst PAMAM dendrimers used in this study.

LA990936P